www.czasopisma.pan.pl PAN POLSKA AKADEMIA NAUK www.journals.pan.pl

PAN ARCHIVES OF ACOUSTICS
Vol. **39**, No. 4, pp. 605–613 (2014)

Copyright © 2014 by PAN – IPPT

DOI: 10.2478/aoa-2014-0065

Control of Bending-Bending Coupled Vibrations of a Rotating Thin-Walled Composite Beam

Jarosław LATALSKI, Marcin BOCHEŃSKI, Jerzy WARMIŃSKI

Department of Applied Mechanics, Lublin University of Technology
Nadbystrzycka 36, 20-618 Lublin, Poland; e-mail: j.latalski@pollub.pl

(*received October 2, 2014; accepted November 14, 2014*)

The paper presents a study of a possible application of structure embedded piezoelectric actuators to enhance the performance of a rotating composite beam exhibiting the coupled flexural-flexural vibrations. The discussed transversal and lateral bending modal coupling results from the directional properties of the beam's laminate and ply stacking distribution. The mathematical model of the beam is based on an assumption of cross-sectional non-deformability and it incorporates a number of non-classical effects. The final 1-D governing equations of an active composite beam include both orthotropic properties of the laminate and transversely isotropic properties of piezoelectric layers. The system's control capabilities resulting from embedded Macro Fiber Composite piezoelectric actuators are represented by the boundary bending moment. To enhance the dynamic properties of the composite specimen under consideration a combination of linear proportional control strategies has been used. Comparison studies have been performed, including the impact on modal coupling magnitude and cross-over frequency shift.

Keywords: thin-walled beam, adaptive materials, feedback control, composite beam, coupled vibrations, structural tailoring.

1. Introduction

The study of the dynamics of rotating beams is an important prerequisite in the design of multiple engineering structures, like turbine and helicopter rotor blades, airplane propellers, flexible robotic arms, etc. This is especially important in the case of systems made of composite materials and multi-layered laminates since they exhibit rich dynamics due to directional properties of fiber reinforced layers. On the other hand, this feature is becoming a promising concept of material tailoring to play a significant role in modern structures design. This refers particularly to advanced mechanical and aerospace designs. Finally, spread of advanced adaptive materials like shape memory alloys, electroactive polymer materials, etc., combined with control strategies open new research areas to further enhance the performance of future systems (Housner *et al.*, 1997).

One of the most promising exemplary application of this technology is an integration of piezoelectric actuators and sensors sub-systems within the master structure – e.g., see review papers by Rao, Sunar (1994) and Sunar, Rao (1999). The adaptive feature is achieved through the converse piezoelectric effect, i.e. the generation of localized strains in response to the voltage applied to the actuator's poles. This induces strain field that changes the dynamic properties of the structure.

Considering anisotropic thin-walled beams, in the past years a number of analytical models and theories of these structures have been proposed and validated. A versatile and comprehensive theory of thin-walled composite beams has been elaborated by e.g. Hodges (2006) and his group – Yu *et al.*, (2005), Kovvali, Hodges (2012); as well as Librescu, Song and their co-workers (Song, Librescu, 1993; 1997; Librescu, Song, 2006). Later on, the studies on thin-walled composite structures done by this group have been extended to smart systems. E.g. (Librescu *et al.*, 1997) analysed the closed-loop natural damped frequencies of anisotropic cantilevered thin-walled beams exhibiting bending-transverse shear twist coupling. The topic has been later continued and extended to blast and

sonic-boom analysis (Libresku, Na, 1998); and next by Song *et al.* (2001) to cases of different modal couplings.

The suggested approach proposes the generation and use of a dynamic moment acting at the tip of the beam. This method, being mathematically elaborated by Lagnese (1989), is referred to as the boundary moment control methodology. In control algorithms this moment is usually related, via a prescribed functional relationship, with one of the various kinematical quantities characterizing the response of the structure (Tzou, Zhong, 1992).

In the presented research the possibility to enhance the dynamic characteristics of a lightweight, cantilevered structures by linking the adaptive capability of smart material and the structural tailoring technology is addressed. The discussed above method of boundary moment control is extended to rotating systems with transverse-lateral bending modal coupling. A control law relating the applied electric field with a linear combination of transverse bending moment at the beam root and free tip rotation measure is implemented. This leads to a boundary value problem to be solved. The submitted study is a further extension of the previous research done by the authors on thin-walled, rotating beams (Latalski *et al.*, 2012; 2014), as well as smart materials and active control strategies Warminski *et al.*, 2011).

2. Structural model and problem formulation

2.1. Beam model

Let us consider a slender, straight and elastic composite, single cell thin-walled beam clamped at the rigid hub of radius R_0 experiencing rotational motion as shown in Fig. 1. The length of the beam is denoted by l, rectangular cross-section characteristic dimensions by c and d, and the wall thickness by h, and it is assumed to be constant spanwise. The composite material is linearly elastic (Hookean) and its properties may vary in orthogonal to the middle surface directions. Two piezoelectric patches are embedded within the laminate top and bottom flanges as shown in Fig. 1c. It is assumed that the piezoelectric material layers are polarized in the thickness direction and exhibit transversely-isotropic properties, the surface of isotropy being normal to the z-direction.

The structural model of the system under consideration incorporates the following kinematic and static assumptions:

1. The original shape of the cross-section is maintained in its plane, but is allowed to warp out of the plane.
2. The concept of the Saint-Venant torsional model is discarded in the favour of the non-uniform torsional one. Therefore, the rate of beam twist $\varphi' = d\varphi/dx$ depends in general on the spanwise coordinate x.
3. In addition to the primary warping effects (related to the cross-section shape), the secondary warping related to the wall thickness is also considered.
4. The transverse beam shear deformations γ_{xy}, γ_{xz} are taken into account. These are assumed to be uniform over the beam's wall cross-section.
5. The stress in walls' transverse normal (σ_{nn}) direction can be neglected; also, due to the prismatic

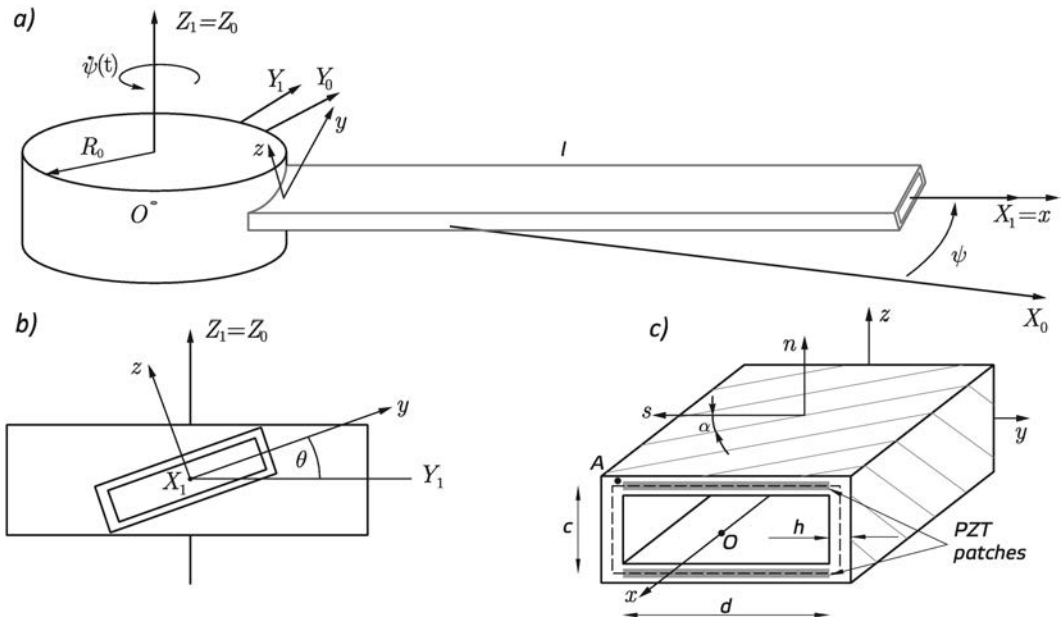

Fig. 1. Rotating thin-walled beam under consideration and reference frames.

beam cross-section, the ratio of the wall thickness to the radius of curvature at any point of the beam's cross-section is zero, therefore, the hoop stress resultant (N_{ss}) is negligible.

6. Both piezoelements embedded in the structure are distributed symmetrically with respect to beam's cross-section mid-line and span the full length of the beam; moreover, it is assumed they are activated simultaneously but out-of-phase.

2.2. Kinematic relations

2.2.1. Displacement field

Following the assumptions given in the previous section the displacements of an arbitrary point A of the cross-section are defined as follows – see for details (Georgiades *et al.*, 2014):

$$\begin{aligned} D_x &= u_0(x,t) + \vartheta_y(x,t)\left(z - n\frac{dy}{ds}\right) \\ &\quad + \vartheta_z(x,t)\left(y + n\frac{dz}{ds}\right) - G(n,s)\varphi'(x,t) \\ &= u_0(x,t) + \vartheta_y(x,t)\,Z + \vartheta_z(x,t)\,Y \\ &\quad - G(n,s)\,\varphi'(x,t), \\ D_y &= v_0\,(x,t) - Y\big(1-\cos\varphi(x,t)\big) - Z\sin\varphi(x,t) \\ &\approx v_0\,(x,t) - \frac{1}{2}Y\big(\varphi(x,t)\big)^2 - Z\varphi(x,t), \\ D_z &= w_0\,(x,t) + Y\sin\varphi(x,t) - Z\big(1-\cos\varphi(x,t)\big) \\ &\approx w_0\,(x,t) + Y\varphi(x,t) - \frac{1}{2}Z\big(\varphi(x,t)\big)^2, \end{aligned} \tag{1}$$

where u_0, v_0, and w_0 are displacements of the point 0 (pole) located on the mid-axis ox and corresponding to the considered one A; $G(s,n)$ is a warping function and $\varphi(x,t)$ denotes beam's twist angle. Angles $\vartheta_y(x,t) = \gamma_{xz} - w_0'$ and $\vartheta_z(x,t) = \gamma_{xy} - v_0'$ represent cross-sections' rotations about respective axes y and z. Moreover, in the above formula the moderately large rotations about ox axis are allowed by the approximation $\cos\varphi \approx 1 - \varphi^2/2$. The later linearisation of the respective resulting equations is performed after incorporation of this approximation.

2.2.2. Strains

Bearing in mind the above displacement relations (1) the following strains formulas can be given:

$$\begin{aligned} \varepsilon_{xx} &= \varepsilon_{xx}^{(0)} + n\varepsilon_{xx}^{(1)} = u_0' + z\vartheta_y' + y\vartheta_z' - G^{(0)}(s)\varphi'' \\ &\quad + \frac{1}{2}(v_0' - z\varphi')^2 + \frac{1}{2}(w_0' + y\varphi')^2 \\ &\quad + n\left(\frac{dz}{ds}\vartheta_z' - \frac{dy}{ds}\vartheta_y' - G^{(1)}(s)\varphi''\right), \end{aligned} \tag{2}$$

$$\begin{aligned} \gamma_{xs} &= \gamma_{xs}^{(0)} + n\gamma_{xs}^{(1)} = (\vartheta_y + w_0')\frac{dz}{ds} + (\vartheta_z + v_0')\frac{dy}{ds}, \\ &\quad + g^{(0)}(s)\varphi' + ng^{(1)}(s)\varphi' \\ \gamma_{xn} &= \gamma_{xn}^{(0)} = -(\vartheta_y + w_0')\frac{dy}{ds} + (\vartheta_z + v_0')\frac{dz}{ds}. \end{aligned} \tag{2}$$

The three remaining strains ε_{yy}, ε_{zz}, γ_{yz} are identically equal to zero due to the cross-section non-deformability assumption.

2.2.3. Velocities

The velocity vector $\dot{\mathbf{R}}$ of an arbitrary point A of the elastic body in the inertial frame $X_0Y_0Z_0$ can be obtained by differentiating its position vector with respect to time. This requires evaluating the time derivative of the transformation matrix. Next, a skew symmetric matrix is defined to formulate an angular velocity vector in a global coordinate system as described in, e.g., Shabana (2005). After appropriate manipulations one arrives at

$$\begin{aligned} \dot{R}_x =& \big[-(D_x + x + R_0)\sin\psi(t) \\ &- (D_y + Y)\cos\theta\cos\psi(t) \\ &+ (D_z + Z)\sin\theta\cos\psi(t)\big]\dot{\psi}(t) \\ &+ \dot{D}_x\cos\psi(t) - \dot{D}_y\cos\theta\sin\psi(t) \\ &+ \dot{D}_z\sin\theta\sin\psi(t), \\ \dot{R}_y =& \big[(D_x + x + R_0)\cos\psi(t) \\ &- (D_y + Y)\cos\theta\sin\psi(t) \\ &+ (D_z + Z)\sin\theta\sin\psi(t)\big]\dot{\psi}(t) \\ &+ \dot{D}_x\sin\psi(t) + \dot{D}_y\cos\theta\cos\psi(t) \\ &- \dot{D}_z\sin\theta\cos\psi(t), \\ \dot{R}_z =& \dot{D}_y\sin\theta + \dot{D}_z\cos\theta, \end{aligned} \tag{3}$$

where overdot means time derivative, so $\dot{D}_x$, $\dot{D}_y$, and $\dot{D}_z$ terms correspond to velocities of deformation.

2.3. Equations of motion

The equations of motion of the rotating beam are derived according to the extended Hamilton's principle of the least action considering both materials – i.e. mono- (laminate) and multi-domain (piezoelectric) one

$$\delta\int_{t_1}^{t_2}\big(\mathcal{L} + \mathcal{W}\big)\,\mathrm{d}t = 0, \tag{4}$$

where $\mathcal{L}$ is the Lagrangian function composed of system's kinetic energy T, potential energy U, and electrical enthalpy $\mathcal{H}$ for linear piezoelectric domain – see, e.g., (Piefort, 2000; Mesecke-Rischmann, 2004); the work of the external forces is given by the $\mathcal{W}$ term.

The kinetic energy of the system is given by

$$T = \frac{1}{2}\int_V \rho\,\dot{\mathbf{R}}^{\mathrm{T}}\,\dot{\mathbf{R}}\,\mathrm{d}V, \tag{5}$$

where designation ρ refers to material density and V refers to the volume element; the potential energy of the elastic system under consideration is given by

$$U = \frac{1}{2}\int_0^l\int_c\int_{-h/2}^{h/2}\left(\sigma_{xx}\varepsilon_{xx} + \sigma_{xn}\gamma_{xn} + \sigma_{xs}\gamma_{xs}\right)\mathrm{d}n\,\mathrm{d}s\,\mathrm{d}x, \tag{6}$$

where appropriate stress terms arise from the classical laminate theory; c in second integral denotes integration along mid-line of the cross-section.

Regarding the electrical enthalpy $\mathcal{H}$ contribution to the overall energy it was shown by Tzou and Zhong (1992) and Librescu *et al.* (1993) that the in-plane isotropic piezoelements that are spread over the entire span of the beam, bonded symmetrically on the opposite faces of the specimen and activated out-of-phase, they generate a bending moment at the beam tip in response to a PZT applied electrical field. This moment does not enter the governing equations and is represented in boundary conditions as a nonhomogeneous term $M_y^{(p)}$ only – see later on Eq. $(9)_2$.

The mentioned in the introductory part of the paper composite structure tailoring technique enables, among other things, the design of a system with requested modal couplings. One of the possible effects in the case of closed section thin-walled beams is flapping-lagging bending transverse shear coupling. As shown by, e.g., (Rehfield *et al.*, 1990; Librescu, Song, 2006) this mode coupling can be achieved by a lamination scheme following the rule $\alpha(z) = \alpha(-z)$, where α denotes the ply angle orientation measured from the circumferential direction axis os being perpendicular to the beam span ox (see Fig. 1c). This scheme is referred to as *Circumferentially Uniform Stiffness* configuration or as *Anti-Symmetric Lay-up Beam* configuration.

Using such a ply-angle lamination scheme and assuming the presetting angle $\theta = 0$ the equations of motion are:

$$\begin{aligned}
&b_1\ddot{v}_0 - b_1 v_0\Omega^2 - b_1\Omega^2[R_x(x)v_0']' - a_{44}(v_0'' + \vartheta_z') - a_{34}\vartheta_y'' = 0,\\
&(b_5 + b_{15})\ddot{\vartheta}_z - (b_5 + b_{15})\Omega^2\vartheta_z - a_{22}\vartheta_z'' - a_{25}(w_0'' + \vartheta_y') + a_{44}(v_0' + \vartheta_z) + a_{34}\vartheta_y' = 0,\\
&b_1\ddot{w}_0 - b_1\Omega^2[R_x(x)w_0']' - a_{55}(w_0'' + \vartheta_y') - a_{25}\vartheta_z'' = 0,\\
&(b_4 + b_{14})\ddot{\vartheta}_y - (b_4 + b_{14})\Omega^2\vartheta_y - a_{33}\vartheta_y'' - a_{34}(v_0'' + \vartheta_z') + a_{55}(w_0' + \vartheta_y) + a_{25}\vartheta_z' = 0,
\end{aligned} \tag{7}$$

and the boundary conditions (geometric) at the beam's root $x = 0$:

$$v = 0, \quad w = 0, \quad \vartheta_y = 0, \quad \vartheta_z = 0, \tag{8}$$

and the dynamic BC at the free end $x = l$:

$$\begin{aligned}
&a_{44}(v_0' + \vartheta_z) + a_{34}\vartheta_y' = 0,\\
&a_{22}\vartheta_z' + a_{25}(w_0' + \vartheta_y) = M_y^{(p)},\\
&a_{55}(w_0' + \vartheta_y) + a_{25}\vartheta_z' = 0,\\
&a_{33}\vartheta_y' + a_{34}(v_0' + \vartheta_z) = 0.
\end{aligned} \tag{9}$$

In the above equations a dot symbol denotes the time derivative and prime symbol corresponds to differentiation with respect to the span coordinate (x). Appearing in the above equations $(7)_1$ and $(7)_3$ terms incorporating

$$R_x(x) = R_0(x - l) + \frac{1}{2}(x^2 - l^2) \tag{10}$$

are contributions to the beam stiffness resulting from the higher order terms in strain field due to centrifugal deformation. Moreover, in the above equations, the Coriolis terms as immaterial ones for the system's dynamics, see (Leissa, Co, 1984) were skipped.

Commenting on the given equations of motion (7) it is worth to emphasize that the modal coupling is achieved by a_{25} and a_{34} terms. These two are different from zero for any fiber orientation angles α except 0° and 90°. It means that for these two specific cases flapping and lagging bendings get fully decoupled.

Details concerning the step-by-step derivation of these equations and calculation of inertia coefficients b_i and stiffness coefficients a_{ij} for the purely laminated beam are given by Georgiades *et al.* (2014) and Song, Librescu (1993). For the system with embedded piezoelements updated formulas at intermediate calculations steps need to be used. Following the approach proposed by Birman (1994) the contribution of piezoelectric material to the overall system stiffness is taken into account in 2-D stretching, bending-stretching, and bending stiffness quantities – A_{ij}, B_{ij}, and D_{ij}, respectively. These are calculated by integration of the reduced elastic coefficients Q_{ij} through the thickness of the multi-layered, non-homogenous wall. After certain mathematical manipulations one arrives at the formula for the boundary bending moment in $(9)_2$ for the discussed case to be

$$M_y^{(p)} = \int_c E_3\frac{h^{(p)}}{2}\delta^{(p)}e_{31}\left[z\left(1 - \frac{A_{12}}{A_{11}}\right) + \frac{dy}{ds}\frac{B_{12}}{A_{11}}\right]\mathrm{d}s, \tag{11}$$

where E_3 is electric field acting solely in the PZT thickness direction and uniform over its volume, $\delta^{(p)}$ is tracker to be equal to 1 for profile flanges, and 0 for profile webs; $h^{(p)}$ is the piezoactuator thickness, and e_{31} is the piezoelectric constant (Song, Librescu, 1996).

It is observed that for the discussed case the piezoelectrically induced boundary bending moment is proportional to the applied electric field. Therefore, for feedback control task, it is convenient to express this

electric field through a prescribed relationship with the mechanical quantities characterizing the beam's response. In the current research the linear combination of bending moment at the beam root and free tip rotation measure is implemented

$$M_y^{(p)} = k_1 \vartheta_y\big|_{x=l} + k_2 \vartheta_y'\big|_{x=0}, \tag{12}$$

where k_1 and k_2 are proportional feedback gains.

2.4. Solution procedure

The solution of the problem is done according to the Extended Galerkin Method. For this purpose the space and time coordinates get separated and problem's unknown variables v_0, w_0, ϑ_y and ϑ_z are written as a sum of linear combinations of the appropriate functions' products

$$v_0(x,t) = \sum_{j=1}^{N} V_j(x)\, q_j(t), \quad \vartheta_y(x,t) = \sum_{j=1}^{N} Y_j(x)\, q_j(t); \tag{13}$$

$$w_0(x,t) = \sum_{j=1}^{N} W_j(x)\, q_j(t), \quad \vartheta_z(x,t) = \sum_{j=1}^{N} Z_j(x)\, q_j(t). \tag{14}$$

In the above $V_j(x)$, $W_j(x)$, $Y_j(x)$, and $Z_j(x)$ are consistent admissible functions which have to fulfill all the geometric boundary conditions while not violating complementary boundary conditions (Baruh, 1999); while $q_j(t)$ are the generalized coordinates. For the discussed problem the trial functions are represented by multiple order polynomials. Substituting the given above approximations (13) and (14) into equations of motion (7) and using appropriate boundary conditions (9), integrating with respect to the spanwise coordinate x one arrives at the algebraic eigenvalue problem

$$\mathbf{M}\ddot{\mathbf{q}} + \mathbf{K}\mathbf{q} = 0, \tag{15}$$

where $\mathbf{q}$ is a $4N$ column matrix whose elements are individual $q_j(t)$ terms and $\mathbf{M}$, $\mathbf{K}$ are $4N \times 4N$ symmetric, square matrices; the control moment $M_y^{(p)}$ (12) formula is included in the $\mathbf{K}$ matrix.

3. Numerical examples and discussion

3.1. Geometry and material data

The geometric characteristics of the rotating beam are displayed below (see also Fig. 1), while the composite material and piezoceramic constants are gathered in Table 1.

$$d = 0.0254 \text{ m}, \quad c = 0.00508 \text{ m}, \quad h = 0.001 \text{ m},$$
$$l = 0.254 \text{ m}, \quad R_0 = 0.1l.$$

Table 1. Graphite epoxy and piezoceramic material data.

Composite material
$E_1 = 206.751 \times 10^9$ Pa, $E_2 = E_3 = 5.17 \times 10^9$ Pa
$G_{12} = G_{13} = 3.11 \times 10^9$ Pa, $G_{23} = 2.55 \times 10^9$ Pa
$\nu_{21} = \nu_{31} = 0.00625$, $\nu_{32} = 0.25$
$\rho = 1528.15$ kg/m^3
Piezoelectric ceramics
$C_{11} = C_{22} = 139.0 \times 10^9$ Pa, $C_{12} = 77.7 \times 10^9$ Pa
$C_{13} = C_{23} = 74.298 \times 10^9$ Pa
$C_{33} = 115.0 \times 10^9$ Pa, $C_{44} = 25.58 \times 10^9$ Pa
$\rho = 7493.9$ kg/m^3

The results from numerical calculations are obtained by the code prepared in Mathematica software. To help in further analysis, plots of stiffness coefficients a_{ij} present in (7) with respect to fiber orientation α are given in Fig. 2. It is clear that for $\alpha = 0°$ and

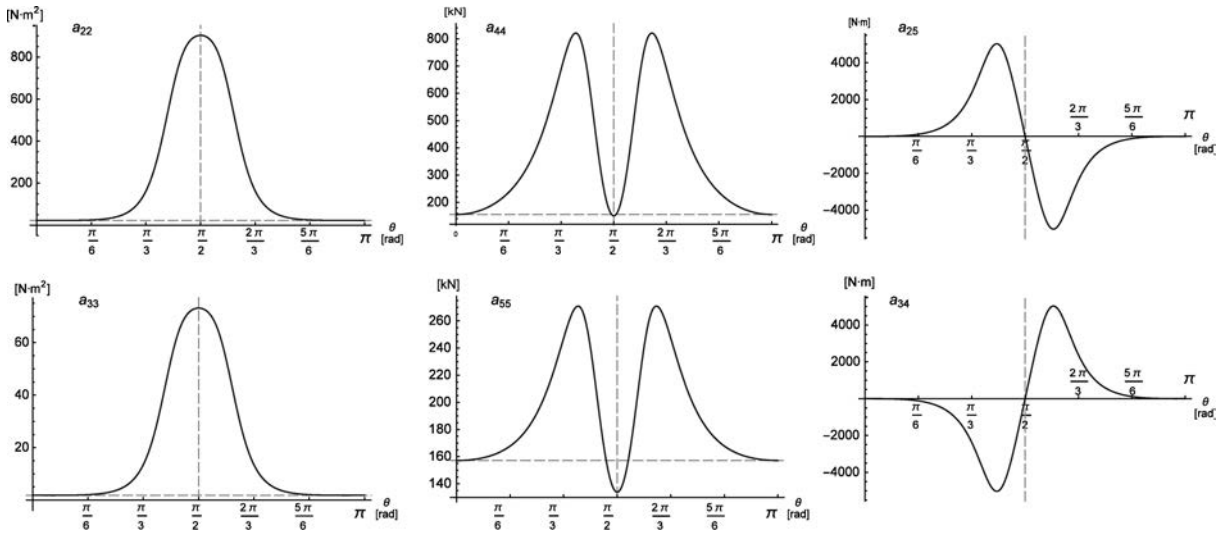

Fig. 2. Stiffness coefficients vs fiber orientation angle; a_{22} – chordwise bending, a_{33} – flapwise bending, a_{44} – chordwise shear, a_{55} – flapwise shear, a_{25} – chordwise bending-flapwise shear, a_{34} – flapwise bending-chordwise shear.

$\alpha = 90°$ both bendings get fully independent; on the other hand, coupling extrema are observed for fibers set at approximately 15° from the beam spanwise direction (i.e., 75° and 105°).

At the next step, the impact of solely presence of piezoactuators on the structure's dynamics is examined (e.g., piezoceramic is embedded in the structure, but the controller is switched-off). Therefore, the Campbell diagram for the first two bending modes is prepared (Fig. 3), while setting the fiber orientation α to 0°. The ω_1 and ω_2 correspond to the flapwise and chordwise bending natural frequencies (these are fully decoupled for $\alpha = 0$), respectively. Capital Ω represents hub rotation frequency. The structure with the actuators is denoted as "piezo", while the one without the actuators is the "raw" one. A strong influence of the actuators' presence to both bending frequencies is visible. This is related to the difference in both materials elastic properties and the significant difference in their densities. Moreover, one can notice the fact that the flapwise frequency is more sensitive to the rotating speed than the chordwise one. This observation is well documented in the literature.

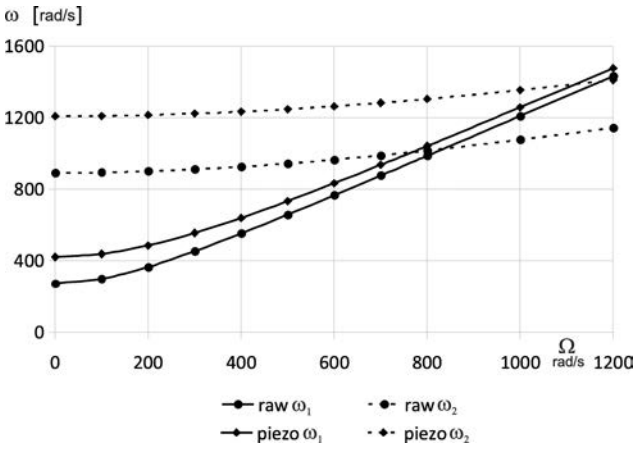

Fig. 3. Campbell diagram for the considered beam; configurations with and without piezoelement are compared.

Figure 4 depicts the open-loop ($\overline{k}_1 = \overline{k}_2 = 0$) and closed-loop ($\overline{k}_1 \neq 0$ or $\overline{k}_2 \neq 0$) eigenfrequencies of the system for selected fiber orientation angles representing weak (a), moderate (b), strong (c) and zero (d) modal coupling cases. While preparing these plots the dimensionless gain coefficients $\overline{k}_1$ and $\overline{k}_2$ were used by normalizing with respect to the beam's length and bending stiffness $a_{33}(\alpha = 0)$ as follows: $\overline{k}_1 = k_1 l^2 / a_{33}|_{(\alpha=0)}$, $\overline{k}_2 = k_2 l / a_{33}|_{(\alpha=0)}$. The solid line corresponds to the first natural frequency ω_1 and the dashed line to the second one ω_2. It is observed that the ω_2 is almost in-sensitive to the control action apart from the fibers' orientation α value. The significant influence of the

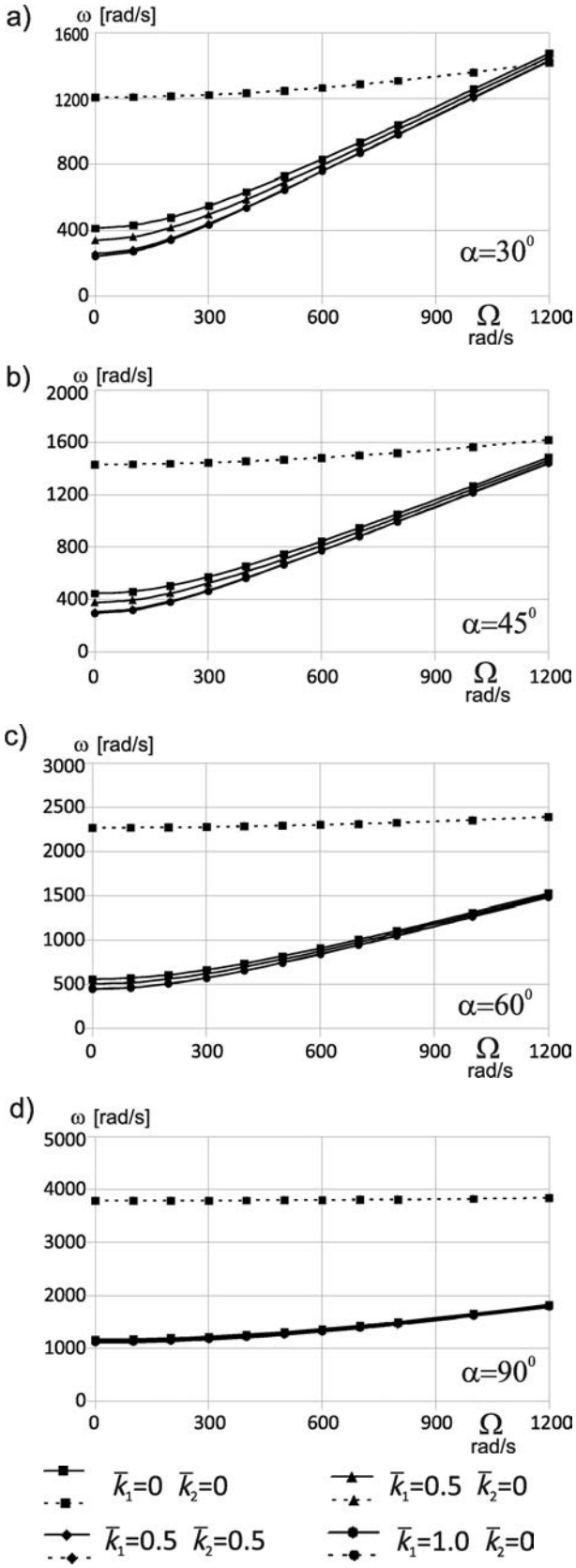

Fig. 4. Campbell diagrams for the controlled beam. Influence of different proportional feedback gains scenarios represented by the $\overline{k}_1$ and $\overline{k}_2$ pairs on eigenfrequencies ω_1 (solid lines) and ω_2 (dashed). Cases of the fibers' orientation α: a) $\alpha = 30°$, b) $\alpha = 45°$, c) $\alpha = 60°$, d) $\alpha = 90°$.

$\overline{k}_1$ and $\overline{k}_2$ values is observed only for a low hub speed Ω and low values of α angle. For α greater than 60° the proportional controller is not efficient. Moreover, for the assumed geometrical and material properties of the structure, its first natural frequency ω_1 is always higher than the hub rotation frequency, independently of the control algorithm and gain.

To consider the case of bending frequencies cross-over ($\omega_1 = \omega_2$), a zoom of one of the diagrams is prepared (Fig. 5). The possibilities to control the position of the crossing point using a proportional feedback are clearly distinctive, although the results for $\overline{k}_1 = 0.5$, $\overline{k}_2 = 0.5$ and $\overline{k}_1 = 1.0$, $\overline{k}_2 = 0$ are similar.

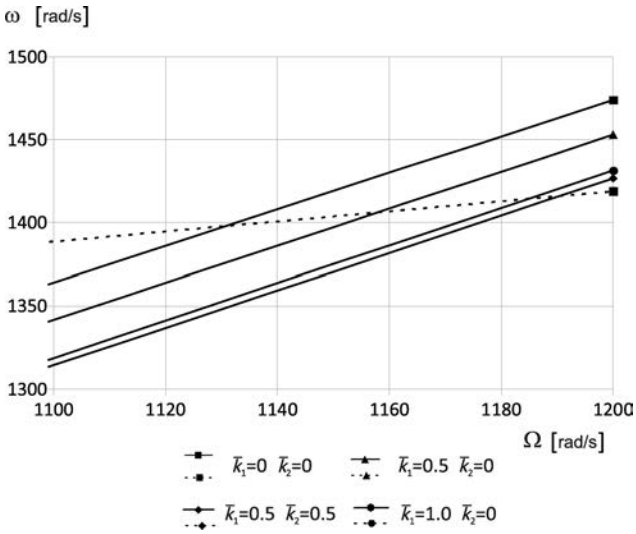

Fig. 5. Zoom of Fig. 4a. Cross-over of ω_1 and ω_2 characteristics for $\alpha = 30°$ and different feedback controls.

Different results for the operation of the considered controllers are observed while the flapwise/chordwise amplitudes ratios are studied – Fig. 6. The significant influence of the $\overline{k}_2$ gain is observed, much stronger than the $\overline{k}_1$ one. This is valid for all fiber orientations α, obviously except the cases $\alpha = 0°$ and $\alpha = 90°$, when both bendings are uncoupled. The efficiency of the proportional controller to change the amplitudes ratio is decreasing while α increases. This is also related to the change in stiffnesses a_{22} and a_{33} with respect to α. This is confirmed in the natural frequencies plot given in Fig. 7.

The obtained results show that for small α values (less than 60°) fibers' orientation is not very significant for the flapwise natural frequency. For higher values this is becoming important and for the limit value $\alpha = 90°$ ω_1 is up to three times higher than for for $\alpha = 45°$. On the other hand, the chordwise natural frequency is obviously dependent on fiber orientation and nearly independent on the hub speed.

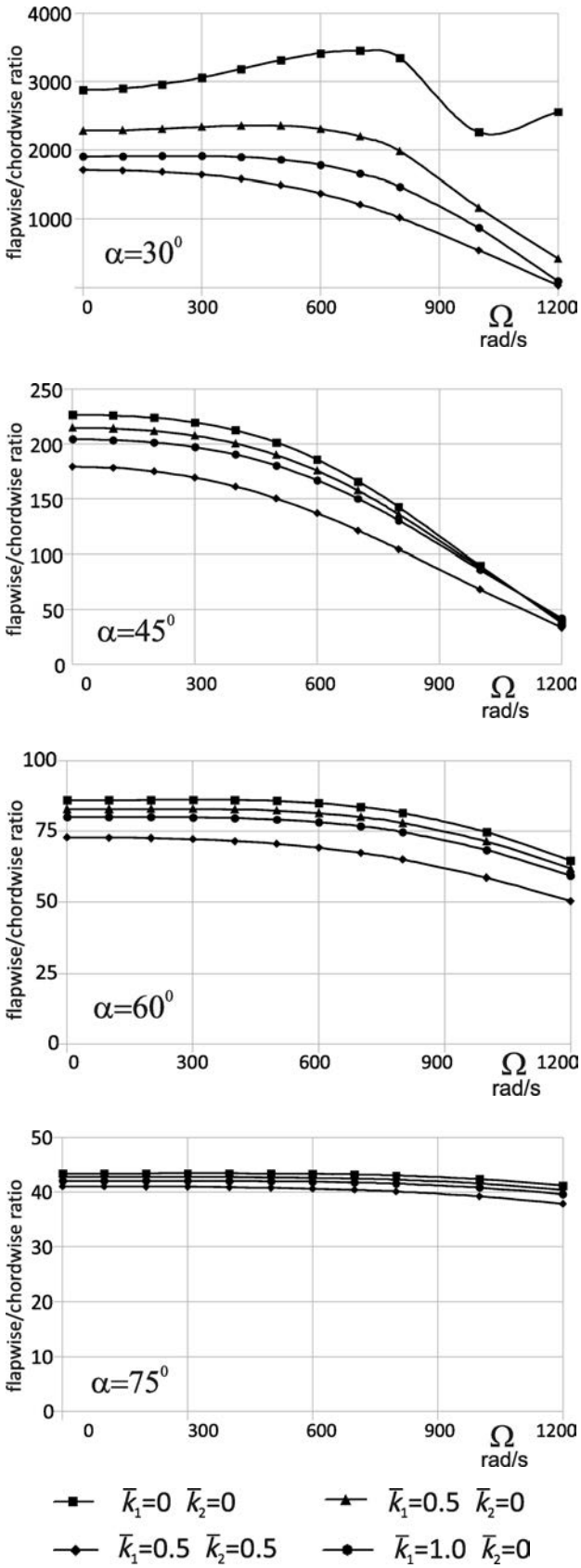

Fig. 6. Influence of different proportional feedback gains scenarios represented by the $\overline{k}_1$ and $\overline{k}_2$ pairs on the flapwise/chordwise amplitudes ratio for selected α fibers' orientations.

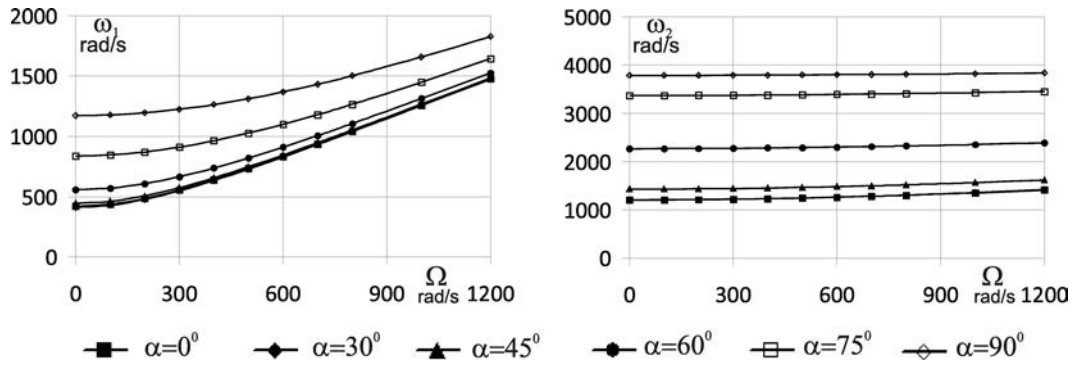

Fig. 7. Beam natural frequencies with respect to the fiber angle α for a system without control.

3.2. Closing remarks

In this article, an investigation of the control of free vibration of thin-walled, rotating cantilever beam has been presented. It is demonstrated that inclusion of thin strips of piezoceramic impact the dynamic characteristics of the system, even without control actions. Next, further possibilities of systems' dynamic characteristics enhancements with the help of the control method are shown. The results highlight the roles played by the discussed feedback control laws for the overall control of beam structures. It is shown that, due to directional properties of a laminate, different effects can be achieved by control methods. Moreover, the outcomes illustrate the capabilities of the adopted feedback control method to shift the cross-over frequency point characteristic for coupled modes dynamics observed in composite rotating beam structures.

Acknowledgment

This research is supported by the Polish National Science Center, research grant No. DEC-2012/07/B/ST8/03931.

References

1. Baruh H. (1999), *Analytical dynamics*, WCB/Mc Graw-Hill, Singapore.
2. Birman V. (1994), *Analytical models of sandwich plates with piezoelectric strip-stiffeners*, International Journal of Mechanical Sciences, **36**, 6, 567–578.
3. Georgiades F., Latalski J., Warmiński J. (2014), *Equations of motion of rotating composite beams with a nonconstant rotation speed and an arbitrary preset angle*, Meccanica, **49**, 8, 1833–1858.
4. Hodges D.H. (2006), *Nonlinear composite beam theory*, Vol. 213 of *Progress in astronautics and aeronautics*, American Institute of Aeronautics and Astronautics.
5. Housner G.W., Bergman L.A., Caughey T.K., Chassiakos A.G., Claus R.O., Masri S.F., Skelton R.E., Soong T.T., Spencer B. F., Yao J.T.P. (1997), *Structural control: Past, present, and future*, Journal of Engineering Mechanics, **123**, 9, 897–971.
6. Kovvali R.K., Hodges D.H. (2012), *Verification of the variational-asymptotic sectional analysis for initially curved and twisted beams*, Journal of Aircraft, **49**, 3, 861–869.
7. Lagnese J. (1989), *Boundary Stabilization of Thin Plates*, SIAM Studies in Applied Mechanics, SIAM, Philadelphia.
8. Latalski J., Bocheński M., Warmiński J., Jarzyna W., Augustyniak M. (2014), *Modelling and simulation of 3 blade helicopter's rotor model*, Acta Physica Polonica A, **125**, 4, 1380–1384.
9. Latalski J., Georgiades F., Warmiński J. (2012), *Rational placement of a macro fibre composite actuator in composite rotating beams*, Journal of Physics: Conference Series, **382**, 1, 012021.
10. Leissa A., Co C. (1984), *Coriolis effects on the vibration of rotating beams and plates*, [in:] Proceedings of the 12th Southeastern Conference on Theoretical and Applied Mechanics, Pine Mountain (GA), USA, pp. 508–513.
11. Librescu L., Meirovitch L., Na S. (1997), *Control of cantilever vibration via structural tailoring and adaptive materials*, AIAA Journal, **35**, 8, 1309–1315.
12. Librescu L., Na S. (1998), *Dynamic response control of thin-walled beams to blast pulses using structural tailoring and piezoelectric actuation*, Journal of Applied Mechanics, **65**, 2, 497–504.
13. Librescu L., Song O. (2006), *Thin-Walled Composite Beams*, Springer.
14. Librescu L., Song O., Rogers C. (1993), *Adaptive vibrational behavior of cantilevered structures modeled as composite thin-walled beams*, International Journal of Engineering Science, **31**, 5, 775–792.
15. Mesecke-Rischmann S. (2004), *Modellierung von flachen piezoelektrischen schalen mit zeverlässigen finiten elementen*, Master's thesis, Institute für Mechanik, Universität der Bundeswehr, Hamburg.
16. Piefort V. (2001), *Finite element modelling of piezoelectric active structures*, Master's thesis, Faculty of Applied Sciences, Université Libre de Bruxelles.

17. Rao S.S., Sunar M. (1994), *Piezoelectricity and its use in disturbance sensing and control of flexible structures: A survey*, Applied Mechanics Reviews, **47**, 4, 113–123.

18. Rehfield L.W., Atilgan A.R., Hodges D.H. (1990), *Nonclassical behavior of thin-walled composite beams with closed cross sections*, Journal of the American Helicopter Society, **35**, 2, 42–50.

19. Shabana A. (2005), *Dynamics of multibody systems*, Cambridge University Press.

20. Song O., Kim J.-B., Librescu L. (2001), *Synergistic implications of tailoring and adaptive materials technology on vibration control of anisotropic thin-walled beams*, International Journal of Engineering Science, **39**, 1, 79–94.

21. Song O., Librescu L. (1993), *Free vibration of anisotropic composite wthin-walled beams of closed cross-section contour*, Journal of Sound and Vibration, **167**, 1, 129–147.

22. Song O., Librescu L. (1996), *Bending vibrations of adaptive cantilevers with external stores*, International Journal of Mechanical Sciences, **38**, 5, 483–498.

23. Song O., Librescu L. (1997), *Structural modeling and free vibration analysis of rotating composite thin-walled beams*, Journal of The American Helicopter Society, **42**, 4, 358–369.

24. Sunar M., Rao S.S. (1999), *Recent advances in sensing and control of flexible structures via piezoelectric materials technology*, Applied Mechanics Reviews, **52**, 1, 1–16.

25. Tzou H.S., Zhong J.P. (1992), *Adaptive piezoelectric structures: Theory and experiment*, [in:] Active Materials and Adaptive Structures – Proceedings of the Proceedings of the ADPA/AIAA/ASME/SPIE Conference, G. Knowels [Ed.], Smart Materials and Structures Series, Institute of Physics, Alexandria (VA), USA, pp. 719–724.

26. Warminski J., Bochenski M., Jarzyna W., Filipek P., Augustyniak M. (2011), *Active suppression of nonlinear composite beam vibrations by selected control algorithms*, Communications in Nonlinear Science and Numerical Simulation, **16**, 5, 2237–2248.

27. Yu W., Hodges D.H., Volovoi V.V., Fuchs E.D. (2005), *A generalized Vlasov theory for composite beams*, Thin-Walled Structures, **43**, 9, 1493–1511.